

Dalton Transactions

Accepted Manuscript



This is an *Accepted Manuscript*, which has been through the Royal Society of Chemistry peer review process and has been accepted for publication.

Accepted Manuscripts are published online shortly after acceptance, before technical editing, formatting and proof reading. Using this free service, authors can make their results available to the community, in citable form, before we publish the edited article. We will replace this *Accepted Manuscript* with the edited and formatted *Advance Article* as soon as it is available.

You can find more information about *Accepted Manuscripts* in the [Information for Authors](#).

Please note that technical editing may introduce minor changes to the text and/or graphics, which may alter content. The journal's standard [Terms & Conditions](#) and the [Ethical guidelines](#) still apply. In no event shall the Royal Society of Chemistry be held responsible for any errors or omissions in this *Accepted Manuscript* or any consequences arising from the use of any information it contains.



Homoleptic octahedral coordination of CH₃CN to Mg²⁺ in the Mg[N(SO₂CF₃)₂]₂-CH₃CN system

Gleb Veryasov, Kazuhiko Matsumoto* and Rika Hagiwara*

Received 00th January 20xx,
Accepted 00th January 20xx

DOI: 10.1039/x0xx00000x

www.rsc.org/

X-ray diffraction and Raman spectroscopic measurements revealed a homoleptic octahedral coordination of CH₃CN to Mg²⁺ in the [Mg(CH₃CN)₆][TFSA]₂ (TFSA = bis(trifluoromethylsulfonyl)imide) crystal structure and in Mg[TFSA]₂/CH₃CN electrolytes.

In addition to improving the commonly used Li-ion batteries, novel batteries are being developed for future applications, especially in large-scale energy devices.¹ Magnesium secondary batteries comprising a magnesium metal negative electrode have higher energy density, improved safety, and lower cost than lithium secondary batteries. Thus, since the report of the first practical cell in 2000 by Aurbach et al.,² they have been considered as attractive candidates for various purposes.^{2-4, 5}

The main challenges in the development of Mg secondary batteries are related to the design of new cathodes and electrolytes.^{3, 6} To date, the most popular electrolytes still lack the necessary requirements to produce a viable product. Etheral solutions of RMgX, Mg(AlCl₃R)₂, and Mg(AlCl₂RR')₂ (R and R' = alkyl or allyl groups) are widely used because they enable stable Mg metal deposition/dissolution behavior.^{2, 5, 7} In addition, magnesium–aluminum chloride complexes provide a wide electrochemical window within the anodic limit of Mg deposition–dissolution.⁸ The Mg source Mg[TFSA]₂ (TFSA =

bis(trifluoromethylsulfonyl)amide) readily dissolves in polar solvents and its Mg²⁺ ions have high affinity to σ-donor ligands.⁶ Its acetonitrile (AN) solution has been examined by several research groups as an electrolyte for Mg secondary batteries.^{3, 6} In 2012, Tran and co-workers investigated in details the use of Mg[TFSA]₂/AN electrolyte for magnesium secondary batteries.⁶ Although the Mg[TFSA]₂/AN electrolyte is not suitable for reversible Mg deposition, its high oxidative stability indicated its potential use as an alternative to Grignard-based electrolytes.⁶ The solution structure plays an important role in electrode reactions and diffusion processes in batteries. However, to the best of our knowledge, there are no experimental reports on the structure of the Mg[TFSA]₂/AN electrolyte; the only computational work by Rajput et al.⁹ was devoted to the investigation of ion pair formation in Mg-based electrolytes. In the present study, we succeeded in isolating high-quality crystals of [Mg(AN)₆][TFSA]₂, which were analyzed

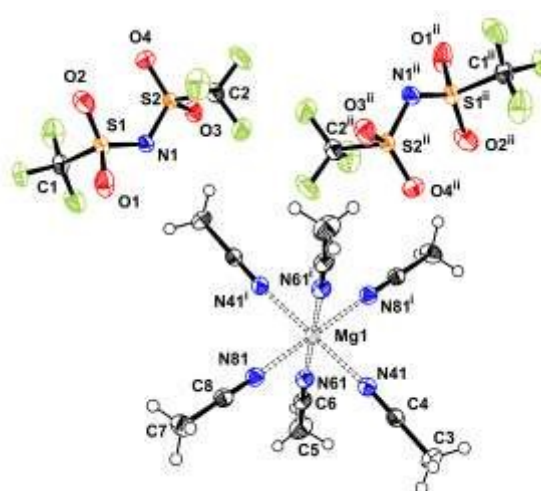


Fig. 1 ORTEP diagram of the [Mg(AN)₆][TFSA]₂ complex. Thermal ellipsoids are drawn at 50% probability. Symmetry operations: (i) 1-x, -y, -z; (ii) 1-x, -y, 1-z. Bond length and angles: Mg1...N41 2.1477(12) Å, Mg1...N61 2.1439(12) Å, Mg1...N81 2.1549(12) Å, N41...Mg1...N61 89.11(5)°, N41...Mg1...N81 90.33(4)°, N61...Mg1...N81 89.81(5)°.

^a Department of Fundamental Energy Science, Graduate School of Energy Science, Kyoto University, Sakyo-ku, Kyoto 606-8501, JAPAN. e-mail: k-matsumoto@energy.kyoto-u.ac.jp, hagiwara@energy.kyoto-u.ac.jp. Tel: +8175-753-5827

[†] Electronic Supplementary Information (ESI) available: Experimental details; Detailed information on X-ray structure determination (Table S1-S2) and Raman spectra recording; Details on D–H...A interactions in [Mg(AN)₆][TFSA]₂ (Fig. S1, Table S3); Packing diagram of [Mg(AN)₆][TFSA]₂ (Fig. S2); List of bands observed in the Raman spectrum of [Mg(AN)₆][TFSA]₂ (Table S4); Raman spectrum of Mg[TFSA]₂ powder (Fig. S3, Table S5); Raman spectrum of the liquid obtained after [Mg(AN)₆][TFSA]₂ crystal melting (Fig. S4); Full-scale Raman spectra of pure acetonitrile and Mg[TFSA]₂–acetonitrile solutions (Fig. S5); Raman spectra of pure acetonitrile, Mg[TFSA]₂–acetonitrile solutions, and [Mg(AN)₆][TFSA]₂; region between 100 and 800 cm⁻¹ (Fig. S6). The CIF file for [Mg(AN)₆][TFSA]₂ can be obtained free of charge from the Cambridge Crystallographic Data Centre via www.ccdc.cam.ac.uk/data_request/cif, CCDC 1437045. See DOI: 10.1039/x0xx00000x

COMMUNICATION

Dalton Transactions

by X-ray diffraction. Raman spectra of this compound and of $\text{Mg}[\text{TFSA}]_2$ -acetonitrile solutions provided detailed insights into the structural properties of $\text{Mg}[\text{TFSA}]_2/\text{AN}$ electrolytes.

Single crystals of $[\text{Mg}(\text{AN})_6][\text{TFSA}]_2$ were grown by fast removal of acetonitrile under dynamic vacuum upon contact of acetonitrile with $\text{Mg}[\text{TFSA}]_2$ (see ESI[†] for more details). The $[\text{Mg}(\text{AN})_6][\text{TFSA}]_2$ crystals easily melt at about room temperature ($\sim 30^\circ\text{C}$); after melting, the compound does not recrystallize. It should be noted that complete dissolution of $\text{Mg}[\text{TFSA}]_2$ in acetonitrile resulted in a transparent homogeneous solution, without any evidence of crystal formation. The obtained $[\text{Mg}(\text{AN})_6][\text{TFSA}]_2$ was extremely hygroscopic and rapidly deliquesced in air. Exposure to air for 2 days resulted in the formation of crystalline materials composed of $[\text{Mg}(\text{H}_2\text{O})_6][\text{TFSA}]_2(\text{H}_2\text{O})_2$, as confirmed by X-ray crystallography.^{10,11} Inclusion of solvents into a crystal lattice was also observed for some alkali and alkaline earth metal salts.^{10,12}

$[\text{Mg}(\text{AN})_6][\text{TFSA}]_2$ crystallizes in the $P2_1/n$ space group with the following parameters: $a = 8.8749(5) \text{ \AA}$, $b = 15.2823(8) \text{ \AA}$, $c = 12.9264(7) \text{ \AA}$, and $\beta = 104.857(2)^\circ$. The ORTEP diagram of the $[\text{Mg}(\text{AN})_6][\text{TFSA}]_2$ complex is shown in Fig. 1. Details of crystal data collection and refinement and selected geometric parameters are given in Tables S1 and S2, ESI[†]). In the coordination sphere of Mg^{2+} , three crystallographically independent acetonitrile molecules form a homoleptic octahedral environment by a crystallographic inversion operation. The $\text{Mg}(\text{AN})_6^{2+}$ moiety is surrounded by eight TFSA^- anions and each anion forms weak $\text{C}\cdots\text{O}$ interactions with acetonitrile molecules, with $\text{H}\cdots\text{O}$ distances varying from 2.50 \AA to 2.67 \AA (VdW radii are 1.20 \AA for H and 1.52 \AA for O;¹³ for more details, see Fig. S1 and Table S3, ESI[†]). These interactions contribute to the formation of a 3D network in which cations and anions are organized in 1D columns (see Fig. S2, ESI[†]).

The TFSA^- anions are known to adopt cis and trans conformations.¹⁴ In the structure of $[\text{Mg}(\text{AN})_6][\text{TFSA}]_2$, these anions adopt a trans conformation, having roughly C_2 symmetry, with $\text{C}\cdots\text{S}\cdots\text{N}\cdots\text{S}$ torsion angles of $109.27(11)^\circ$ and $94.10(12)^\circ$ for $\text{C1}\cdots\text{S1}\cdots\text{N1}\cdots\text{S2}$ and $\text{C2}\cdots\text{S2}\cdots\text{N1}\cdots\text{S1}$, respectively. The formation of $\text{Mg}(\text{AN})_6^{2+}$ has been previously observed in the structures of $[\text{Mg}(\text{AN})_6][\text{Sb}_2\text{Cl}_8]^{15}$ and $[\text{Mg}(\text{AN})_6][\text{Bi}_4\text{Cl}_{16}]^{16}$. The $\text{Mg}\cdots\text{N}$ distances are 2.1439(12) \AA , 2.1477(12) \AA , and 2.1549(12) \AA for the three crystallographically independent acetonitrile molecules and are comparable with those reported (2.134(7)–2.179(8) \AA) for $[\text{Mg}(\text{AN})_6][\text{Sb}_2\text{Cl}_8]^{15}$ and slightly shorter than those (2.20(2)–2.25(3) \AA) observed in the structure of $[\text{Mg}(\text{AN})_6][\text{Bi}_4\text{Cl}_{16}]^{16}$.

The weak $\text{C}\cdots\text{H}\cdots\text{O}$ interactions between acetonitrile molecules and TFSA^- anions may prevent crystallization from the completely dissolved acetonitrile solution of $\text{Mg}[\text{TFSA}]_2$. Because the mixing of $\text{Mg}[\text{TFSA}]_2$ and acetonitrile in a 1:6 ratio led to the formation of $[\text{Mg}(\text{AN})_6][\text{TFSA}]_2$ with homoleptic $\text{Mg}(\text{AN})_6^{2+}$, higher levels of acetonitrile are expected to generate a similar Mg coordination sphere. Formation of $[\text{Mg}(\text{H}_2\text{O})_6][\text{TFSA}]_2(\text{H}_2\text{O})_2$ owing to the final water consumption process indicates that the $\text{Mg}^{2+}\cdots\text{OH}_2$ bond energy is higher than that of $\text{Mg}^{2+}\cdots\text{NCCH}_3$, and even small amounts of

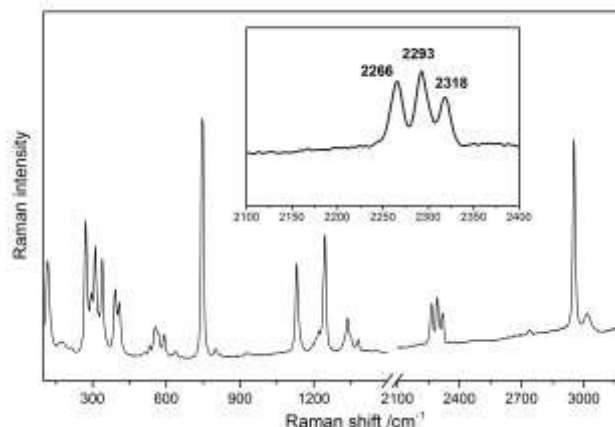


Fig. 2 Raman spectrum of $[\text{Mg}(\text{AN})_6][\text{TFSA}]_2$. The magnified fragment shows three $\nu(\text{C}\equiv\text{N})$ bands.

water form strongly bonded hydrates.

The Raman spectrum of $[\text{Mg}(\text{AN})_6][\text{TFSA}]_2$, shown in Fig. 2, was recorded on a single crystal, confirmed by X-ray diffraction and sealed in a 0.5 mm glass capillary under dry atmosphere (for details, see Table S4, ESI[†]). The assignments were made based on literature data,¹⁷ and the Raman spectrum of pure $\text{Mg}[\text{TFSA}]_2$ powder was used for the identification of the TFSA^- anion band (see Fig. S3 and Table S5 ESI[†]). The characteristic frequency of coordination compounds containing acetonitrile is the $\text{C}\equiv\text{N}$ stretching vibration, denoted as $\nu(\text{C}\equiv\text{N})$. In the spectrum of $[\text{Mg}(\text{AN})_6][\text{TFSA}]_2$, three $\nu(\text{C}\equiv\text{N})$ bands at 2266, 2293, and 2318 cm^{-1} were detected. This splitting can be interpreted by considering normal coordinate analysis for octahedral species (A_{1g} and E_g) and factor group splitting (lowering of symmetry from O_h to C_i).¹⁸ In pure acetonitrile,¹⁹ this band appears at 2249 cm^{-1} and is expected to shift toward higher or lower frequencies depending on the nature of the moiety.²⁰ In the IR spectrum of $[\text{Mg}(\text{AN})_6][\text{Bi}_4\text{Cl}_{12+2x}]^{16}$ $\nu(\text{C}\equiv\text{N})$ appeared as a doublet at 2322 and 2290 cm^{-1} for $x = 2$ and at 2320 and 2289 cm^{-1} for $x = 3$. The most intense band in the $\text{Mg}[\text{TFSA}]_2$ and $[\text{Mg}(\text{AN})_6][\text{TFSA}]_2$ spectra corresponds to the combination of $\delta_s(\text{CF}_3)$ and $\nu_s(\text{SNS})$ vibrations (see assignments in Table S5, ESI[†])²¹ at 754 and 748 cm^{-1} , respectively. The position of this band related to Mg^{2+} was discussed by Watkins et al.²¹ (also in the case of Li^+ by Umebayashi et al.²²); its appearance at higher frequencies indicates a stronger bonding of the anion to the metal core. Because there is no $\text{Mg}^{2+}\cdots\text{TFSA}^-$ contact in $[\text{Mg}(\text{AN})_6][\text{TFSA}]_2$, the $\delta_s(\text{CF}_3) + \nu_s(\text{SNS})$ band appears at a frequency that is 6 cm^{-1} lower than that of pure $\text{Mg}[\text{TFSA}]_2$. According to previous reports, the $\nu(\text{Mg}\cdots\text{N})$ and $\omega(\text{Mg}\cdots\text{NCC})$ (ω = wagging) bands are supposed to appear at 340–350 cm^{-1} and 250–255 cm^{-1} , respectively.^{16, 23} The $\omega(\text{Mg}\cdots\text{NCC})$ bands are too weak to be detected in the present spectrum; moreover, $\nu(\text{Mg}\cdots\text{N})$ overlaps with the $\tau(\text{SO}_2)$ (τ = torsion) band at 338 cm^{-1} (see Fig. S3, ESI[†]).

The spectrum of the liquid obtained after $[\text{Mg}(\text{AN})_6][\text{TFSA}]_2$ crystal melting is shown in Fig. S4, ESI[†]. The three $\nu(\text{C}\equiv\text{N})$

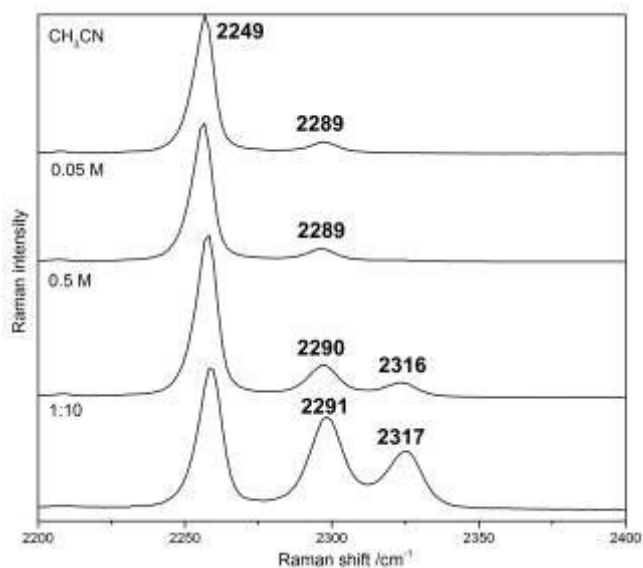


Fig. 3 Raman spectra of pure acetonitrile and acetonitrile solutions of Mg[TFSA]₂ (0.05 M, 0.5 M, and 1:10) between 2200 and 2400 cm⁻¹.

stretching bands are retained and the $\delta_s(\text{CF}_3) + \nu_s(\text{SNS})$ band, deriving from TFSA⁻, appeared at 742 cm⁻¹, indicating a weaker bonding of the anionic species than that in the original crystal. Thus, we can conclude that, in the liquid state of [Mg(AN)₆][TFSA]₂, the homoleptic Mg(AN)₆²⁺ unit is retained.

In order to investigate the coordination sphere of Mg²⁺ in Mg[TFSA]₂/AN electrolytes, three acetonitrile solutions of Mg[TFSA]₂, i.e., 1:10, 0.5 M, and 0.05 M, were prepared for Raman spectroscopic analysis. Mass balance calculations show that the 0.5 and 0.05 M solutions correspond to Mg[TFSA]₂:acetonitrile molar ratios of 1:33 and 1:227, respectively. Full-scale spectra are shown in Fig. S5, ESI[†]. Because the relative intensity of the bands assigned to the coordination sphere of TFSA⁻ and Mg²⁺ for the 0.05 M solution was too low (below 1% of the intensity of the $\nu(\text{C}\equiv\text{N})$ band of free acetonitrile) to be distinguished from the background, the properties of this solution are not discussed here (see Fig. 3 and Fig. S5, ESI[†]).

The $\nu(\text{C}\equiv\text{N})$ region of the recorded spectra is shown in Fig. 3. The intensities are normalized to the band at 2249 cm⁻¹ ($\nu(\text{C}\equiv\text{N})$ of free acetonitrile). The band at 2289 cm⁻¹ in the spectrum of pure acetonitrile is due to the combination of ν_3 ($\xi(\text{C}-\text{H})$, ξ = twisting) and ν_4 ($\nu(\text{C}-\text{C})$) normal modes, according to Westlund and co-authors.²⁴ Analogously to [Mg(AN)₆][TFSA]₂, the acetonitrile solutions of Mg[TFSA]₂ show three bands in this region. In all spectra, one band appears at the same position as the $\nu(\text{C}\equiv\text{N})$ band of pure acetonitrile and is presumably due to acetonitrile molecules that are not coordinated to Mg²⁺. The peak found at 2266 cm⁻¹ in the spectrum of the [Mg(AN)₆][TFSA]₂ crystal does not appear in the spectra of the acetonitrile solutions of Mg[TFSA]₂. The other two bands are assigned to the $\nu(\text{C}\equiv\text{N})$ of the acetonitrile molecules coordinated to Mg²⁺, corresponding to A_{1g} and E_g modes under O_h symmetry. The ratio of the three Raman band areas for the 1:10 solution can be roughly approximated as

4:3:3. However, precise peak fitting is difficult because of combinational band contributions to the total peak areas; e.g., $\nu_3 + \nu_4$ band at 2289 cm⁻¹, which should appear together with $\nu(\text{C}\equiv\text{N})$ at 2291 cm⁻¹. This may suggest that, of the ten acetonitrile molecules, six are coordinated to Mg²⁺ and the remaining four are in the free state.

The appearance of only two $\nu(\text{C}\equiv\text{N})$ bands from the homoleptic Mg(AN)₆²⁺ unit in solution may be due to the mobility of the TFSA⁻ anions. In contrast to the [Mg(AN)₆][TFSA]₂ complex with three crystallographically independent acetonitrile molecules, in the Mg(AN)₆²⁺ units in solution, only two different states occur for acetonitrile molecules in the Mg(AN)₆²⁺ units in solution.

Another feature of the acetonitrile solutions of Mg[TFSA]₂ is the characteristic conformation of the TFSA⁻ anions. In a previous work, the barrier between the cis and trans conformations of TFSA⁻ was determined to be 2.2–3.3 kJ mol⁻¹,²⁵ which easily enables the transition. Fujii et al. investigated the Raman spectra of the cis conformer in solution, with the aid of computational chemistry.²⁵ In the [EMI][TFSA] (EMI = 1-ethyl-3-methylimidazolium) ionic liquid, the $\omega(\text{SO}_2)$ band, which serves as a fingerprint of the conformation of TFSA⁻ anions, appears at 398 cm⁻¹ and 407 cm⁻¹ for the trans and cis conformations, respectively.²⁵ In the Raman spectrum of [Mg(AN)₆][TFSA]₂, the band at 408 cm⁻¹ (see Fig. S6, ESI[†]) is assigned to the $\omega(\text{SO}_2)$ vibration (see Table S4, ESI[†]). This band is shifted to higher frequencies than that in [EMI][TFSA] because of the effect of the C–H...O interactions. The same band appears at 405 cm⁻¹ in the 1:10 and 0.5 M solutions, indicating that the TFSA⁻ anions adopt a trans conformation in solution as well (see Fig. S5, ESI[†]). It is noteworthy that, in the spectrum of the [Mg(AN)₆][TFSA]₂ crystal, the band at 393 cm⁻¹, assigned to $\delta(\text{C}-\text{C}-\text{N})$, where δ denotes bending, shifts to a higher frequency than the literature data for pure acetonitrile.¹⁹ This shift is not observed in the Raman spectra of the liquid samples, and the band appears at 378 cm⁻¹ for both 0.5 M and 1:10 solutions. This indicates that acetonitrile molecules are not immobilized by the C–H...O interactions with the TFSA⁻ anions because of the mobility of the TFSA⁻ anions in the liquid state.

The $\nu(\text{Mg}\cdots\text{O})$ band was reported to appear at around 250 cm⁻¹ in the Raman spectrum of the Mg[TFSA]₂-[BMPyr][TFSA] (BMPyr = *N*-butyl-*N*-methylpyrrolidinium) ionic liquid.²¹ This band was not observed in the spectrum of the acetonitrile solution of Mg[TFSA]₂ and presumably corresponds to the peak at 259 cm⁻¹ in the spectrum of pure Mg[TFSA]₂ powder (see Fig. S3 and Table S5). The $\delta_s(\text{CF}_3) + \nu_s(\text{SNS})$ band (discussed above for pure Mg[TFSA]₂ powder and [Mg(AN)₆][TFSA]₂ adduct) appeared at 741 cm⁻¹ in the 1:10 solution and at 739 cm⁻¹ in the 0.5 M solution. This supports the absence of bonding between the TFSA⁻ anions and Mg²⁺ ions in solution.

The results of this study show that, in acetonitrile solutions of Mg[TFSA]₂, Mg²⁺ is in a homoleptic octahedral coordination with acetonitrile molecules. Raman spectroscopy revealed the mobility of the TFSA⁻ anions, which adopt a trans conformation in both [Mg(AN)₆][TFSA]₂ salt and

COMMUNICATION

Dalton Transactions

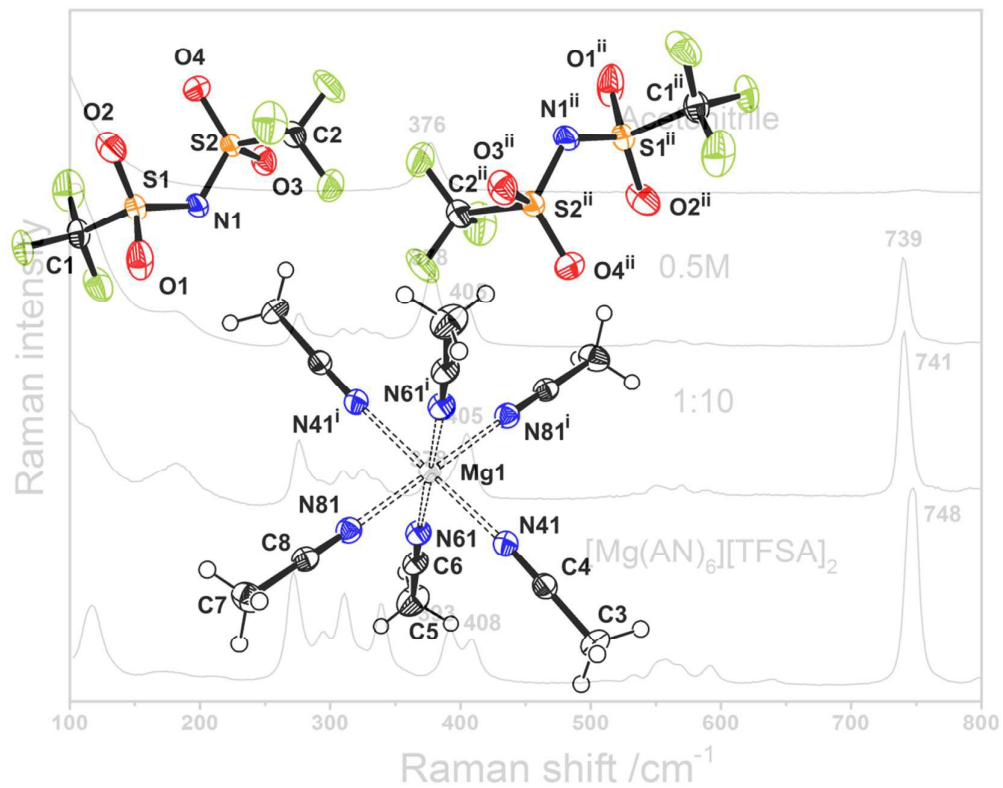
Mg[TFSA]₂-acetonitrile solutions. In a recent report, Rajput et al. performed a computational study of solvation in different Mg-based electrolytes,⁹ including the Mg[TFSA]₂/AN system. Radial distribution functions for the cation–cation, cation–anion, and cation–solvent pairs obtained by molecular dynamics simulation allowed them to conclude that Mg²⁺⋯TFSA⁻ interaction is dominant compared with the Mg²⁺-acetonitrile interaction.⁹ However, our investigation strongly suggested that Mg²⁺ ions form an entity with six acetonitrile molecules and Mg²⁺⋯TFSA⁻ interaction does not occur.

Acknowledgements

This work was financially supported by the Grant-in-Aid for Scientific Research of Japan Society for the Promotion of Science, #26-04763.

Notes and references

1. M. Armand and J. M. Tarascon, *Nature*, 2008, **451**, 652-657.
2. D. Aurbach, Z. Lu, A. Schechter, Y. Gofer, H. Gizbar, R. Turgeman, Y. Cohen, M. Moshkovich and E. Levi, *Nature*, 2000, **407**, 724-727.
3. Y. Orikasa, T. Masese, Y. Koyama, T. Mori, M. Hattori, K. Yamamoto, T. Okado, Z.-D. Huang, T. Minato, C. Tassel, J. Kim, Y. Kobayashi, T. Abe, H. Kageyama and Y. Uchimoto, *Sci. Rep.*, 2014, **4**, 5622.
4. H. D. Yoo, I. Shterenberg, Y. Gofer, G. Gershinsky, N. Pour and D. Aurbach, *Energy Environ. Sci.*, 2013, **6**, 2265-2279; Y. Kumar, S. A. Hashmi and G. P. Pandey, *Electrochim. Acta*, 2011, **56**, 3864-3873; E. Levi, Y. Gofer and D. Aurbach, *Chem. Mater.*, 2010, **22**, 860-868; F.-f. Wang, Y.-s. Guo, J. Yang, Y. Nuli and S.-i. Hirano, *Chem. Commun.*, 2012, **48**, 10763-10765; J. Muldoon, C. B. Bucur, A. G. Oliver, T. Sugimoto, M. Matsui, H. S. Kim, G. D. Allred, J. Zajicek and Y. Kotani, *Energy Environ. Sci.*, 2012, **5**, 5941-5950; R. Mohtadi, M. Matsui, T. S. Arthur and S.-J. Hwang, *Angew. Chem. Int. Ed.*, 2012, **51**, 9780-9783; H. S. Kim, T. S. Arthur, G. D. Allred, J. Zajicek, J. G. Newman, A. E. Rodnyansky, A. G. Oliver, W. C. Boggess and J. Muldoon, *Nat. Commun.*, 2011, **2**, 427.
5. M. Matsui, *J. Power Sources*, 2011, **196**, 7048-7055.
6. T. T. Tran, W. M. Lamanna and M. N. Obrovac, *J. Electrochem. Soc.*, 2012, **159**, A2005-A2009.
7. G. Cheng, Q. Xu, M. Zhang, F. Ding, X. Liu and L. Jiao, *Chin. Sci. Bull.*, 2013, **58**, 3385-3389; D. Aurbach, A. Schechter, M. Moshkovich and Y. Cohen *J. Electrochem. Soc.*, 2001, **148**, A1004-A1014; Q. Zhao, Y. NuLi, T. Nasiman, J. Yang and J. Wang, *Int. J. Electrochem.*, 2012, **2012**.
8. R. E. Doe, R. Han, J. Hwang, A. J. Gmitter, I. Shterenberg, H. D. Yoo, N. Pour and D. Aurbach, *Chem. Commun.*, 2014, **50**, 243-245.
9. N. N. Rajput, X. Qu, N. Sa, A. K. Burrell and K. A. Persson, *J. Am. Chem. Soc.*, 2015, **137**, 3411-3420.
10. L. Xue, D. D. DesMarteau and W. T. Pennington, *Solid State Sciences*, 2005, **7**, 311-318.
11. A. Haas, C. Klare, P. Betz, J. Bruckmann, C. Krüger, Y. H. Tsay and F. Aubke, *Inorg. Chem.*, 1996, **35**, 1918-1925.
12. L. Xue, C. W. Padgett, D. D. DesMarteau and W. T. Pennington, *Solid State Sciences*, 2002, **4**, 1535-1545.
13. A. Bondi, *J. Phys. Chem.*, 1964, **68**, 441-451.
14. P. Johansson, S. P. Gejji, J. Tegenfeldt and J. Lindgren, *Electrochim. Acta*, 1998, **43**, 1375-1379.
15. M. G. B. Drew, P. P. K. Claire and G. R. Willey, *J. Chem. Soc., Dalton Trans.*, 1988, 215-218.
16. G. R. Willey, H. Collins and M. G. B. Drew, *J. Chem. Soc., Dalton Trans.*, 1991, 961-965.
17. M. Herstedt, M. Smirnov, P. Johansson, M. Chami, J. Grondin, L. Servant and J. C. Lassègues, *J. Raman Spectrosc.*, 2005, **36**, 762-770; I. Rey, P. Johansson, J. Lindgren, J. C. Lassègues, J. Grondin and L. Servant, *J. Phys. Chem. A*, 1998, **102**, 3249-3258; M. Castriota, T. Caruso, R. G. Agostino, E. Cazzanelli, W. A. Henderson and S. Passerini, *J. Phys. Chem. A*, 2005, **109**, 92-96.
18. K. Nakamoto, in *Infrared and Raman Spectra of Inorganic and Coordination Compounds*, John Wiley & Sons, Inc., 2008, 1-273.
19. T. Shimanouchi, *Tables of Molecular Vibrational Frequencies Consolidated*, National Bureau of Standards, 1972.
20. D. P. Fairlie, W. G. Jackson, B. W. Skelton, H. Wen, A. H. White, W. A. Wickramasinghe, T. C. Woon and H. Taube, *Inorg. Chem.*, 1997, **36**, 1020-1028; R. E. Clarke and P. C. Ford, *Inorg. Chem.*, 1970, **9**, 227-235.
21. T. Watkins and D. A. Buttry, *J. Phys. Chem. B*, 2015, **119**, 7003-7014.
22. Y. Umebayashi, T. Mitsugi, S. Fukuda, T. Fujimori, K. Fujii, R. Kanzaki, M. Takeuchi and S.-i. Ishiguro, *J. Phys. Chem. B*, 2007, **111**, 13028-13032.
23. J. Reedijk and W. L. Groeneveld, *Recl. Trav. Chim. Pays-Bas*, 1968, **87**, 1079-1088.
24. J. C. Evans and H. J. Bernstein, *Can. J. Chem.*, 1955, **33**, 1746-1755; P.-O. Westlund and R. M. Lynden-Bell, *Mol. Phys.*, 1987, **60**, 1189-1209.
25. K. Fujii, T. Fujimori, T. Takamuku, R. Kanzaki, Y. Umebayashi and S.-i. Ishiguro, *J. Phys. Chem. B*, 2006, **110**, 8179-8183.



The Mg^{2+} ion in the $\text{Mg}[\text{N}(\text{SO}_2\text{CF}_3)_2]_2\text{-CH}_3\text{CN}$ system is surrounded by six acetonitrile molecules in both the solid and liquid states.